AEM
Journals.ASM.org

Microbial Lithotrophic Oxidation of Structural Fe(II) in Biotite

Evgenya Shelobolina,[a] Huifang Xu,[a,b] Hiromi Konishi,[a,b] Ravi Kukkadapu,[c] Tao Wu,[a] Marco Blöthe,[a] and Eric Roden[a,b]

Department of Geoscience, University of Wisconsin—Madison, Madison, Wisconsin, USA[a]; NASA Astrobiology Institute, University of Wisconsin—Madison, Madison, Wisconsin, USA[b]; and Pacific Northwest National Laboratory, Richland, Washington, USA[c]

Microorganisms are known to participate in the weathering of primary phyllosilicate minerals through the production of organic ligands and acids and through the uptake of products of weathering. Here we show that the lithotrophic Fe(II)-oxidizing, nitrate-reducing enrichment culture described by Straub et al. (K. L. Straub, M. Benz, B. Schink, and F. Widdel, Appl. Environ. Microbiol. 62:1458–1460, 1996) can grow via oxidation of structural Fe(II) in biotite, a Fe(II)-rich trioctahedral mica found in granitic rocks. Oxidation of silt/clay-sized biotite particles was detected by a decrease in extractable Fe(II) content and simultaneous nitrate reduction. Mössbauer spectroscopy confirmed structural Fe(II) oxidation. Approximately 1.5×10^7 cells were produced per μmol of Fe(II) oxidized, in agreement with previous estimates of the growth yield of lithoautotrophic circumneutral-pH Fe(II)-oxidizing bacteria. Microbial oxidation of structural Fe(II) resulted in biotite alterations similar to those found in nature, including a decrease in the unit cell b dimension toward dioctahedral levels and Fe and K release. Structural Fe(II) oxidation may involve either direct enzymatic oxidation, followed by solid-state mineral transformation, or indirect oxidation as a result of the formation of aqueous Fe, followed by electron transfer from Fe(II) in the mineral to Fe(III) in solution. Although it is not possible to distinguish between these two mechanisms with available data, the complete absence of aqueous Fe in oxidation experiments favors the former alternative. The demonstration of microbial oxidation of structural Fe(II) suggests that microorganisms are directly responsible for the initial step in the weathering of biotite in granitic aquifers and the plant rhizosphere.

Microbial populations below the Earth's surface constitute a substantial portion of the Earth biosphere (36) and could potentially exert a significant influence on global geochemistry, including the weathering of primary minerals in the Earth's crust. Two dominant rocks in the Earth's crust, basalt and granite, contain ferrous iron [Fe(II)] that could serve as an energy source for microorganisms that gain energy from lithotrophic metabolism. Basaltic rocks are found primarily in the oceanic crust, and the importance of the Fe(II) derived from the dissolution of basaltic glass for lithoautotrophic microbial biomass production has been postulated (2) and studied in detail (25).

Biotite, a Fe(II)-rich trioctahedral mica, is the main source of structural Fe(II) in granitic rocks and accounts for a significant fraction of the exposed continental crust surface (18). Biotite weathering is a source of K for plant nutrition and a major source of Fe and Mg in groundwater (5). At circumneutral pH, biotite weathering involves the oxidation of structural Fe(II) and the exchange of interlayer K for ions in the external solution, while at acidic pH it proceeds through incongruent dissolution (37). The known modes of microbial mediation of biotite weathering include the production of acids and ligands and cation uptake, which together promote mineral dissolution subsequent to the oxidation of structural Fe(II) (29). However, to date, the ability of microorganisms to participate in the initial step of biotite weathering, i.e., structural Fe(II) oxidation, has not been evaluated. The only three silicate minerals demonstrated to date to serve as Fe(II) sources for microbial Fe(II) oxidation at near-neutral pH are the nesosilicates almandine and strautolite (11) and the secondary phyllosilicate smectite (27).

In this study, we examined the potential of the structural Fe(II) in biotite to support the metabolism of lithotrophic microorganisms. The experiments were carried out with a robust lithoautotrophic Fe(II)-oxidizing, nitrate-reducing enrichment culture described by Straub et al. (31). This culture (referred to here as the Straub culture) is dominated by a betaproteobacterium 94 to 95% similar in 16S rRNA gene sequence to the known neutrophilic, chemolithoautotrophic Fe(II)-oxidizing organisms "*Sideroxydans lithotrophicus*" strain ES-1 and *Gallionella ferruginea* (7). The Straub culture is capable of aqueous Fe(II) oxidation coupled to the reduction of nitrate to N_2, with CO_2 serving as the sole source of carbon (7, 31). This culture can also oxidize solid-phase Fe(II)-bearing minerals such as siderite and magnetite (33). Unlike other members of the family *Gallionellaceae*, the Straub culture prefers nitrate rather than oxygen as the electron acceptor.

MATERIALS AND METHODS

Biotite. Biotite from Bancroft, Ontario, Canada (Ward Scientific, 46-1190), or Murray Bay, Quebec, Canada (University of Wisconsin collection 8131), was used in microbial biotite oxidation experiments. The composition of the biotite specimen was determined with a Cameca SX51 electron microprobe with mineral standards. The oxidation state of Fe in Bancroft biotite was calculated based on the Mössbauer spectrum. The biotite from Bancroft biotite contained 16.29% FeO and had a composition of $(K_{0.980}, Na_{0.025})$ $(Fe^{2+}_{0.996}, Fe^{3+}_{0.222}, Mg_{1.663}, Ti_{0.117})$ $(Si_{3.048}, Al_{0.812}, Ti_{0.140})$ O_{10} $(OH_{1.02}, F_{0.98})$. The biotite from Murray Bay contained 18.32% FeO and had a composition of $(K_{0.949}, Na_{0.028})$ $(Fe_{1.254}, Mg_{0.733}, Mn_{0.010}, Al_{0.559}, Ti_{0.131})$ $(Si_{2.826}, Al_{1.174})$ O_{10} $(OH)_2$.

Large crystals of biotite were ground in a ceramic mortar and then

Received 30 March 2012 Accepted 29 May 2012
Published ahead of print 8 June 2012
Address correspondence to Evgenya Shelobolina, shelobolina@wisc.edu.
Supplemental material for this article may be found at http://aem.asm.org/.

doi:10.1128/AEM.01034-12

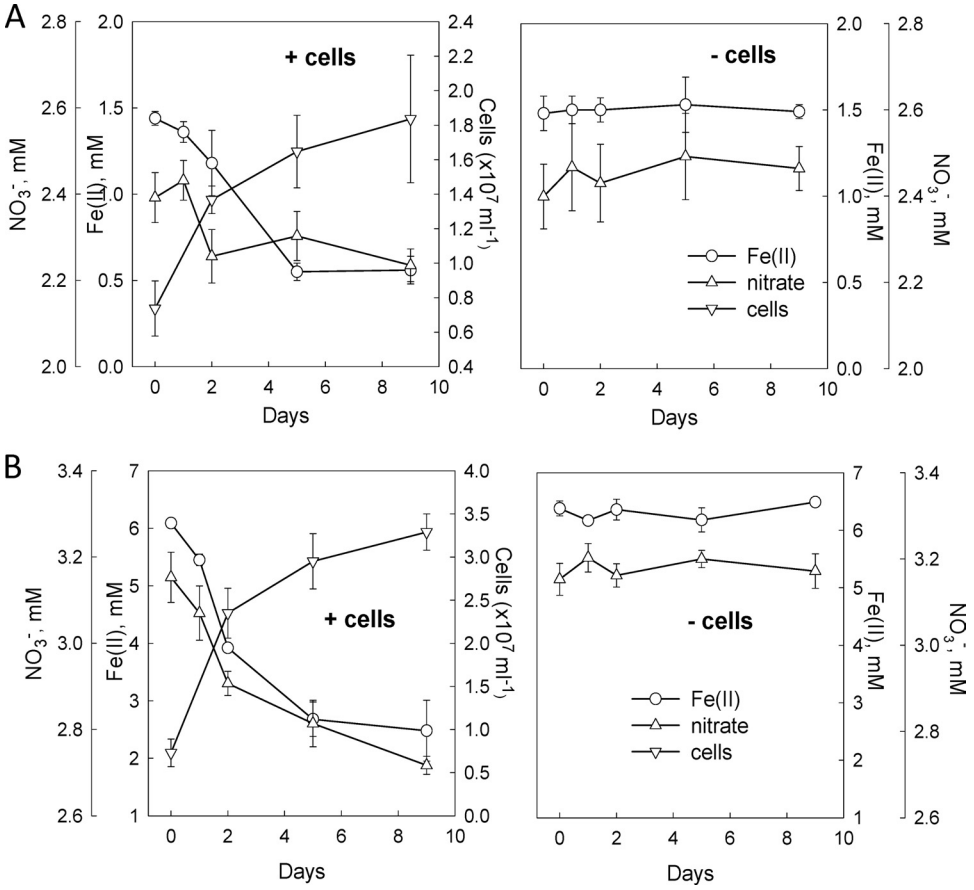

FIG 1 Growth and metabolism of the Straub culture with Bancroft (A) or Murray (B) biotite as the electron donor and nitrate as the electron acceptor. The results are the means of triplicate cultures.

sieved to yield flakes with a particle size below 45 μm. Biotite flakes with a particle size below 45 μm were used to obtain a detailed growth curve (see Fig. 3). The <5-μm-size fraction was separated from the coarser mineral grains by centrifugation and decantation. The settling time for the <5-μm-size fraction was calculated for a particle density of 3.1 g/cm^3 using Stokes' law. Biotite stock suspensions were prepared by adding biotite particles to distilled water at a concentration 15 to 20 g/liter, bubbling with N_2, and sterilization by autoclaving. Biotite flakes with a particle size below 5 μm were used for all experiments except a detailed microbial growth experiment on Bancroft biotite (see Fig. 3). The volume of biotite stock suspension added to the medium was adjusted in order to provide 1.5 to 7 mmol/liter 0.5 M HCl-extractable Fe(II).

Microbial culture. The Straub culture was provided by K. L. Straub to E. E. Roden in 1998 for use in studies of nitrate-dependent oxidation of solid-phase Fe(II) compounds (33) and has been maintained in the Roden laboratory since that time. Strict anaerobic techniques were used throughout. An anoxic bicarbonate-buffered medium with a final pH of 6.8 contained (g/liter) $NaHCO_3$ (2.5), NH_4Cl (0.25), and $NaH_2PO_4 \cdot H_2O$ (0.06). Medium was dispensed into 25-ml pressure tubes under N_2-CO_2 (80:20). The tubes were capped with butyl rubber stoppers and sterilized by autoclaving. The culture was maintained on medium containing 10 mM soluble Fe(II) ($FeCl_2$) and 5 mM nitrate. No reducing agent was used. In all of the experiments reported here (except controls with no electron donor), biotite was used as the sole electron donor source with 5 mM nitrate as the electron acceptor. Biotite cultures were inoculated with a portion (5%, vol/vol) of a freshly grown $FeCl_2$/nitrate culture in which >95% Fe(II) oxidation had taken place.

Analytical techniques. All sampling of cultures was performed using sterile anoxic techniques. In all experiments but that in which a detailed growth curve was determined (see Fig. 3), oxidation of Fe(II) in biotite was monitored by determining changes in the amount of Fe(II) released after 12 h of extraction of whole culture samples (biotite, cells, and solution) with 0.5 M HCl, followed by Fe(II) analysis using ferrozine (16). In the experiment presented in Fig. 3, the sample was centrifuged in the anaerobic chamber to separate the liquid and solid phases. Centrifugation and removal of the supernatant were necessary to avoid potential Fe(II) oxidation by biogenic nitrite under acidic conditions during HCl extraction. The liquid-phase sample was analyzed for nitrate, nitrite, Fe, and K. The solid-phase sample was analyzed for 0.5 M HCl-extractable and HF-extractable Fe. Unfortunately, neither 0.5 M HCl nor hydrofluoric acid extraction, followed by Fe(II) analysis using 1,10-phenanthroline analysis (32), completely recovered the total Fe(II) content of the biotite. However, both extraction procedures provide a suitable means to quantify microbial Fe(II) oxidation, and parallel analyses of culture samples by both methods gave comparable results (see Fig. 3). The total Fe content of the biotite was determined after dissolution in 29 M HF. Aqueous Fe and K were measured by inductively coupled plasma (ICP) analysis. Aqueous samples were acidified to prevent Fe loss from the solution. Nitrate and nitrite concentrations were measured by ion chromatography. Cells were counted with 4′,6-diamidino-2-phenylindole (DAPI) staining and epifluorescence microscopy (15).

TEM. Transmission electron microscopy (TEM) analyses were carried out with microbially oxidized and control biotite at the final time point (14 days) of the experiment shown in Fig. 3 using an FEI Titan 80-200 aberration-corrected scanning/transmission electron microscope associated with an EDAX AMETEK high-resolution energy-dispersive X-ray spectroscopy (EDS) detector and a Gatan image-filtering system and operated at 200 kV. The samples were mixed with distilled water and ultra-

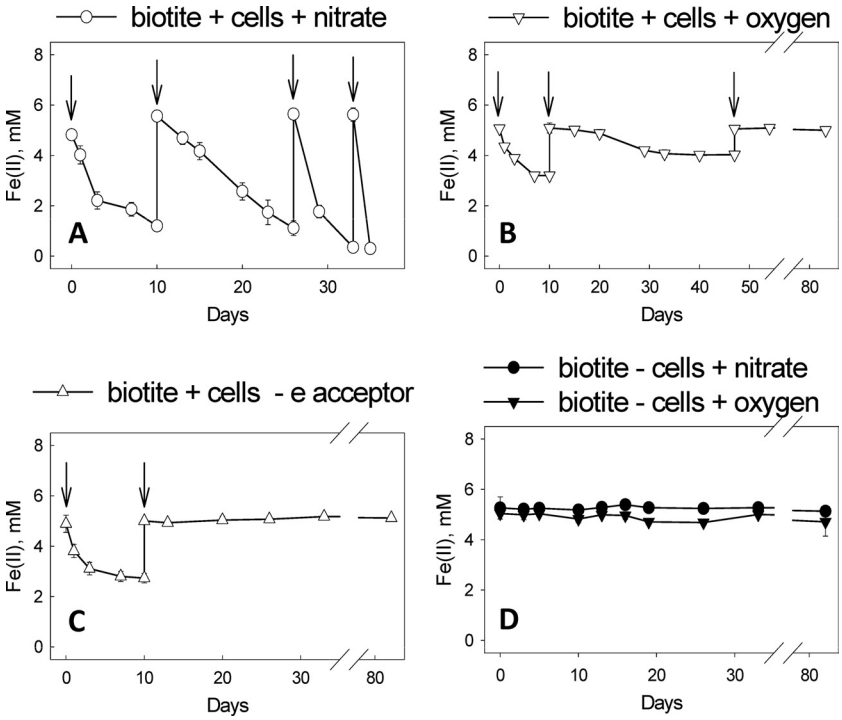

FIG 2 Changes in 0.5 M HCl-extractable Fe(II) content during multiple generations of the Straub culture. Arrows designate 10% transfer of the culture into fresh medium. (A) Bancroft biotite and nitrate; (B) Bancroft biotite and oxygen; (C) Bancroft biotite with no added electron acceptor; (D) sterile (uninoculated) medium with Bancroft biotite and nitrate or oxygen.

sonicated for ~3 min. A drop of the resulting suspension was placed on a lacey-carbon-coated Cu grid and air dried.

XRD. X-ray diffraction (XRD) analyses were carried out with microbially oxidized and control biotite at the final time point (14 days) of the experiment shown in Fig. 3 using a Rigaku Rapid II X-ray diffraction system with a two-dimensional image plate (Mo K-alpha radiation). Diffraction data were collected on an image plate detector. The two-dimensional images were then integrated to produce conventional 2-theta intensity patterns using Rigaku's 2DP software. The instrument used an accelerating voltage of 50 kV, a current of 50 mA, an exposure time of 15 min, and a 0.1-mm-diameter collimator. Biotite particles were mixed with a small amount of distilled water, and the resulting paste was mounted on the end of a glass fiber and air dried.

Mössbauer spectroscopy. ^{57}Fe transmission Mössbauer spectroscopy was employed to characterize the Fe mineralogy of the microbially oxidized and control (unoxidized) biotite at the final time point (14 days) of the experiment shown in Fig. 3. Mössbauer spectra were collected at various temperatures, from room temperature to liquid helium temperature, using a 75-mCi (initial strength) ^{57}Co/Rh source. The velocity transducer used (MVT-1000; WissEL) was operated in a constant-acceleration mode (23 Hz, ±12 mm/s). An Ar-Kr proportional counter was used to detect the radiation transmitted through the holder. Data were folded to give a flat background and a zero-velocity position corresponding to the center shift of a metal Fe foil at room temperature. Calibration spectra were obtained with a 25-μm-thick Fe(m) foil (Amersham, Amersham, England). The Mössbauer data were modeled with Recoil software (University of Ottawa, Ottawa, Ontario, Canada) (22). Although thickness correction of the samples was not carried out, identical experimental conditions (e.g., Lorentzian half width at half maximum, 0.1 mm/s) and sample amounts (100 mg in a sample holder with a 0.5-inch outside diameter) were used to obtain optimal comparison of the microbially oxidized and control samples.

RESULTS AND DISCUSSION

Fe(II) oxidation in biotite. The ability of the Straub culture to grow by oxidation of Fe(II) in biotite was first examined with two biotite specimens of different chemical compositions, including Bancroft biotite and Murray biotite (Fig. 1). Growth of the culture in anaerobic, nitrate-amended fine silt/clay-sized biotite slurries resulted in a decrease in Fe(II) content and simultaneous nitrate consumption. Growth ceased after 9 days of incubation when ca. 5% of the total Fe(II) content of the biotite was oxidized. In the slurry of Bancroft biotite, oxidation of 0.89 mmol/liter of 0.5 M HCl-extractable Fe(II) resulted in the reduction of 0.16 mM nitrate and the production of 1.24×10^7 cells/ml. In the slurry of Murray biotite, oxidation of 3.61 mmol/liter of 0.5 M HCl-extractable Fe(II) resulted in the reduction of 0.44 mM nitrate and the production of 2.56×10^7 cells/ml. These data correspond to ratios of 0.18 and 0.12 mol of nitrate consumed per mol of Fe(II) oxidized, lower than the ratio of 0.2 expected for the denitrification-based metabolism of this culture (7, 31). This result may be explained by the partial sorption of nitrate to biotite surfaces (6). The cell yield was 1.4×10^7 cells per μmol of Fe(II) oxidized in both experiments. No Fe(II) loss or nitrate consumption was observed in control slurries without microorganisms.

More detailed studies linking microbial Fe(II) oxidation to mineralogical changes were performed with Bancroft biotite. The Straub culture was able to repeatedly (three consecutive culture generations) oxidize Fe(II) in a suspension of Bancroft biotite with nitrate as the electron acceptor but not in the presence of oxygen or when no electron acceptor was added. (Fig. 2A to C). There was no noticeable Fe(II) oxidation in mineral suspensions

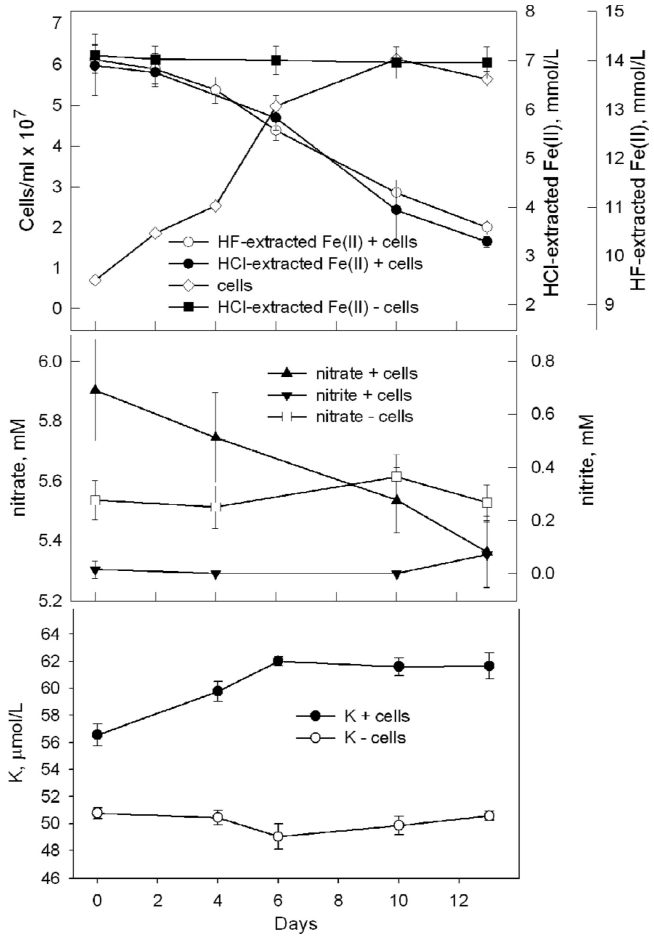

FIG 3 Growth of the Straub culture with biotite as the sole source of energy and nitrate as the electron acceptor. Each datum point represents the mean of triplicate cultures.

lacking the culture (Fig. 2D). A detailed growth experiment was conducted using an inoculum that had been grown previously in biotite-nitrate medium (Fig. 3). Approximately 3 mmol/liter Fe(II) was oxidized in 10 days as measured by both 0.5 M HCl extraction and HF extraction, which corresponded to about 5% of the total Fe(II) content of the mineral suspension. Consumption of nitrate (ca. 0.4 mM) and an increase in the cell density (5.4×10^7 cells/ml) took place in conjunction with Fe(II) oxidation. The ratio of nitrate reduced to Fe(II) oxidized was 0.13, similar to that observed in the experiments shown in Fig. 1. The cell yield was 1.8×10^7 cells per μmol of Fe(II) oxidized, similar to the yields in the first experiments with Bancroft biotite and Murray biotite (Fig. 1) and to cell yields determined previously for this (7, 11, 17) and other (19, 30) known neutrophilic Fe(II)-oxidizing bacteria. Mössbauer spectroscopy provided independent confirmation of structural Fe(II) oxidation in microbially oxidized biotite (Fig. 4A). Modeling of the room temperature spectra (see Fig. S1 and Table S1 in the supplemental material) suggested ca. 6% oxidation, in a good agreement with the chemical extraction data.

Mineralogical changes in microbially oxidized biotite. Previous observations of biotite weathering in nature state that Fe(II) oxidation in biotite should result in decreases in K and Fe contents and a shift in the unit cell b dimension toward dioctahedral levels (26). The expulsion of some K and Fe from the structure is caused by the positive charge excess in the octahedral sheet when structural Fe(II) is oxidized to Fe(III). The increase in the structural Fe(III) content of weathered biotite results in a gradual transformation of the trioctahedral sheet of biotite (characterized by a higher unit cell b dimension) into a dioctahedral sheet (characterized by a lower unit cell b dimension). In addition, the partial conversion of a tri- to a dioctahedral structure can be accompanied by distortion of the tetrahedral sheet configuration from a hexagon-like ring to a di-trigonal ring (3), resulting in stacking disorder.

To test if these phenomena occurred in our system, the time course of K and Fe in the liquid phase of growing biotite cultures was examined by ICP analysis, and the solid phase of grown biotite cultures was examined by high-resolution TEM and X-ray diffraction. A small release of K (ca. 5 μmol/liter) above the background in sterile controls was detected in the liquid phase of the microbially oxidized biotite slurries (Fig. 3). No aqueous Fe (ICP analysis; detection limit, < 0.05 μM; data not shown) was detected at any time in either inoculated or sterile suspensions. However, nanometer size particles were found along the edges of the surface steps

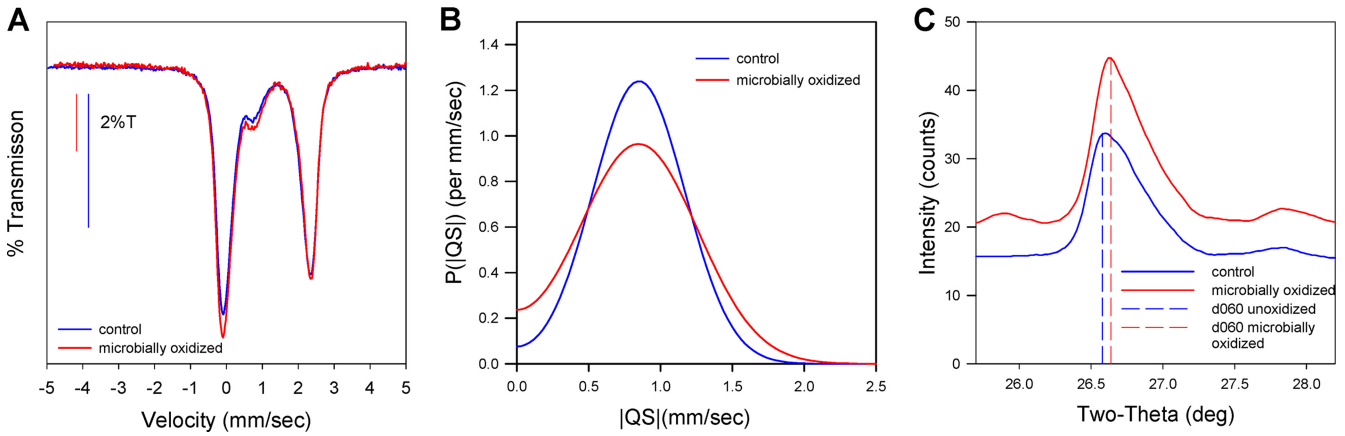

FIG 4 Mössbauer and XRD spectra of control versus microbially oxidized biotite. (A) Room temperature Mössbauer spectra of the control (blue) versus microbially oxidized (red) biotite; (B) quadrupole splitting distributions of Fe(III) sites; (C) 060 XRD peaks. Note the d_{060} spacing change from 1.542 Å to 1.539 Å in the microbially oxidized sample (see Fig. S3 in the supplemental material for overall XRD patterns).

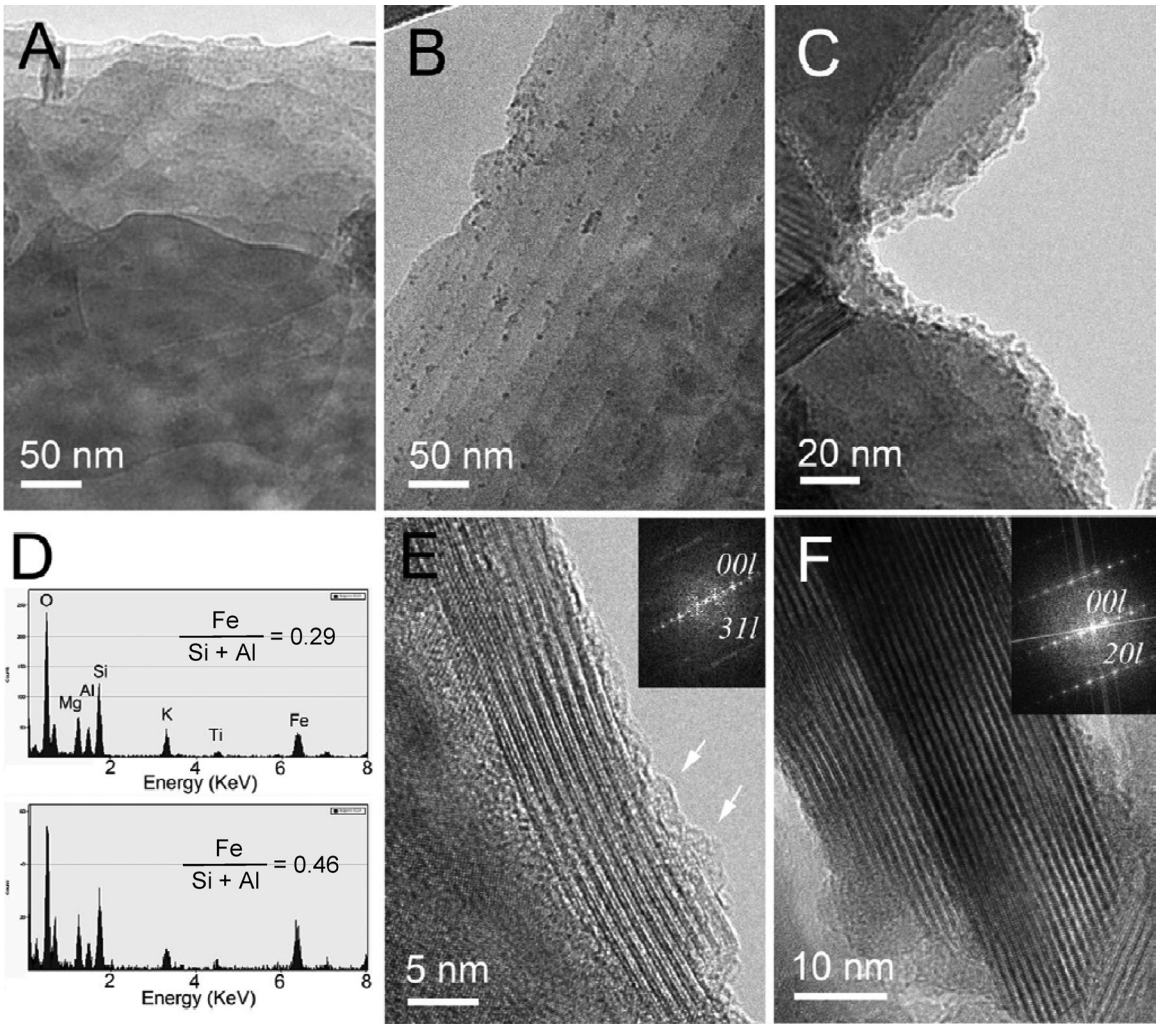

FIG 5 TEM analysis of control versus microbially oxidized biotite. Shown are bright-field TEM images of the clean biotite plate surface in the control (A) and spotty amorphous Fe(III) oxyhydroxide precipitates along the surface steps and edge of a microbially oxidized sample (B, C). Also shown are X-ray EDS spectra (D) showing Fe enrichment [as indicated by the Fe/(Si+Al) atomic ratio] from a Fe(III) oxyhydroxide precipitate on the microbially oxidized biotite surface (lower spectrum) compared to a neighboring area without precipitates (upper spectrum). HTEM images and Fourier transform patterns indicate stacking disordering in the microbially oxidized biotite plates (E) and an ordered stacking structure in the control (F) based on streaking or sharp non-00l spots in the inserted Fourier transform patterns. The two arrows in panel E indicate Fe(III) oxyhydroxide precipitate on the biotite surface.

of the microbially oxidized biotite (Fig. 5B and C). X-ray EDS demonstrated that the area at the edges of the microbially oxidized biotite were enriched in Fe compared to the bulk mineral substrate (Fig. 5D), suggesting that the linear dots visible in Fig. 5B and C are early-stage amorphous Fe(III) oxyhydroxides. Under the circumneutral pH conditions of our cultures, any Fe released from the biotite structure would be expected to precipitate immediately as an insoluble Fe(III) oxyhydroxide phase. Two potential mechanisms of Fe release from the biotite structure can be envisioned. One is that culture does not produce any Fe-complexing agents and Fe is expelled from the biotite structure as a result of the positive charge excess in the octahedral sheet when structural Fe(II) is oxidized to Fe(III) (by a solid-state mineral transformation process) (26). Another potential mechanism is that some Fe is solubilized and reprecipitated by the culture in close association with biotite particles. In this case, no soluble Fe would be detected in solution as well. We cannot distinguish between these two mechanisms with the available data, but this represents an important next step in understanding both the fundamental mechanism of enzymatic oxidation of biotite (see below) and the contribution of enzymatic Fe(II) oxidation to biotite weathering in nature.

It was more common to see stacking disorder (streaks in the Fourier transform pattern) in microbially oxidized biotite than in unoxidized biotite (Fig. 5E and F). X-ray diffraction analysis of microbially oxidized versus unoxidized biotite (Fig. 4D) showed a slight shift of the 060 diffraction peak toward a higher angle corresponding to a decrease in d_{060} spacing and the unit cell b dimension due to Fe(II) oxidation and partial release of Fe. This shift is consistent with an observed broadening of the arbitrary quadrupole splitting distribution of the Mössbauer Fe(III) doublet upon oxidation (Fig. 4B), which implies redox-induced changes in local symmetries of biotite (21). The liquid He temperature Mössbauer spectral features of the control biotite are in good agreement with a prior Mössbauer analysis of biotite that showed Fe(III) sextets as well as peaks attributable to magnetically ordered Fe(II) and paramagnetic Fe(III) and Fe(II) (see Fig. S2 in the supplemental ma-

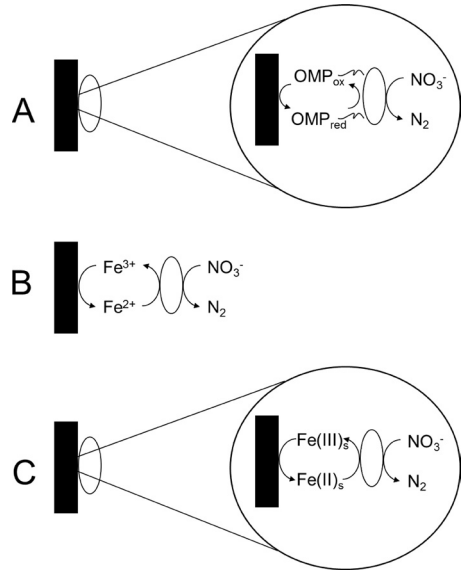

FIG 6 Conceptual models of potential mechanisms of biotite oxidation by the Straub culture (cells are depicted as ovals). (A) Direct enzymatic attack, e.g., extracellular solid-phase electron transfer analogous to that involved in neutral-pH microbial reduction of insoluble Fe(III) oxides; OMP represents an outer membrane protein involved in electron transfer. (B) Indirect oxidation through dissolution followed by electron transfer between Fe(III) in solution and structural Fe(II) in biotite. (C) Indirect oxidation in which surface-bound Fe(III) atoms [Fe(III)$_s$] function in a manner analogous to Fe(III) in solution, leading to the formation of sorbed Fe(II) [Fe(II)$_s$] produced through electron exchange between surface Fe(III) and the structural Fe(II) in biotite.

terial) (21). The relatively greater contribution of sextet B in the microbially oxidized sample than in the control confirmed Fe(II) oxidation, in agreement with the room temperature data. The nature of sextet B and its quantitative contribution to the overall liquid He spectrum, however, are not certain. The detection by TEM of small amounts of Fe-enriched nanosized particles along the edges of the microbially oxidized biotite (Fig. 5B) suggests that the sextet B peaks could be due to nanoparticulate Fe(III) oxyhydroxide. In light of the small percentage of Fe(II) oxidation, however, a distinct contribution of these peaks to the overall spectrum would not be expected, and the sextet B peaks cannot be unequivocally assigned to Fe(III) oxyhydroxide.

Mechanism of Fe(II) oxidation in biotite. Although the mineralogical and chemical analyses clearly demonstrated that oxidation of structural Fe(II) in biotite took place, the mechanism whereby the Straub culture oxidized structural Fe(II) cannot be precisely defined. A few basic scenarios can be envisioned, as illustrated in Fig. 6. One is a direct enzymatic attack (Fig. 6A), e.g., extracellular solid-phase electron transfer analogous to that involved in neutral-pH microbial reduction of insoluble Fe(III) oxides and Fe(III)-bearing phyllosilicates (14). A second is indirect oxidation through dissolution (e.g., through the production of Fe-complexing agents, as mentioned above in the context of Fe mobilization from the biotite structure), followed by electron transfer between Fe(III) in solution and solid-phase Fe(II) (Fig. 6B) (35). Another possibility is that once coatings of nanoparticulate Fe(III) oxide form on biotite, the surface-bound Fe(III) atoms function in a manner analogous to Fe(III) in solution. In this case, the cells would attack the biotite indirectly through oxidation of the sorbed Fe(II) that was produced as a result of electron exchange between surface Fe(III) and structural Fe(II) in the biotite (Fig. 6C). An analogous process (albeit in the opposite direction in terms of the flow of electrons) was recently described for the interaction between Fe(II) sorbed on the surface of Fe(III)-bearing smectite, where the sorbed Fe(II) was shown to transfer electrons to the underlying structural Fe(III) (24). It is important to emphasize that the processes depicted in Fig. 6 are ones that occur prior to the Fe/K expulsion and associated mineral transformation reactions that take place subsequent to Fe(II) oxidation, i.e., the well-known pathways of oxidative biotite weathering at neutral pH (37).

In nature, direct Fe(II) oxidation is likely to take place in circumneutral, low-organic-matter subsurface environments, such as deep granitic aquifers. In contrast, the indirect dissolution-based mechanism (24, 35) is likely to be important at subneutral pH or in the presence of Fe(III)-binding ligands, i.e., conditions typical of surface soils (including the plant rhizosphere).

Implications for granitic rock weathering. The well-known modes of microbial mediation of biotite weathering, including production of acids and ligands and cation uptake (29), are restricted to photosynthetically driven, organic-rich environments, such as lichen-colonized exposed rocks and the plant rhizosphere (4). However, the vast majority of environments where biotite oxidative weathering takes place are not directly supported by photosynthesis. A key example is subsurface regolith formation from granitic rocks (9, 13), where inputs of organic matter are orders of magnitude lower than in near-surface environments (10).

Although caution is required in extrapolating the results of our short-term laboratory experiments with ground and autoclaved biotite to processes that occur in granitic aquifers (12, 28), the ability of a lithotrophic culture to use structural Fe(II) in biotite as an electron donor suggests a mechanism by which lithotrophic microbial communities in the deep subsurface could sustain themselves in the absence of major photosynthetically derived carbon input. Pedersen (20) proposed that the granitic biosphere is fueled by hydrogen that supports the growth of methanogenic and acetogenic organisms as primary producers in this ecosystem. Despite the fact that members of the family *Gallionellaceae* have been repeatedly documented in granitic aquifers (1, 20, 23), structural Fe(II) in primary phyllosilicates was believed to be refractory and has not been previously considered a potential electron donor for microbial metabolism. The results of our study suggest that lithotrophic microorganisms capable of oxidizing structural Fe(II) in biotite could serve as an alternative energetic base of a granitic microbial ecosystem when oxygen or nitrate is available as an electron acceptor. This situation would represent a terrestrial analog to reduced Fe-based chemolithoautotrophic microbial communities that inhabit basalt rock environments on the seafloor (25).

Implications for biotite weathering in the rhizosphere. The results of this study also suggest an additional mechanism of microbial biotite weathering in the rhizosphere, an ecologically important process that contributes to soil formation and provides K and Fe for plant nutrition. The accepted model of biotite weathering in the rhizosphere is proton attack as a result of microbial production of organic and inorganic acids (8), followed by removal of the products of weathering (cations dissolved from the mineral) by the production of complex-forming agents (organic acids, EPS, siderophores) and/or by cellular cation uptake (34).

Instead of or in addition to proton attack, microbial Fe(II) oxidation could accelerate the initial step in the weathering process. Studies of biotite weathering under organic-rich conditions typical of the rhizosphere, in the presence and absence of structural Fe(II)-oxidizing microorganisms, are required to evaluate the potential significance of this phenomenon.

ACKNOWLEDGMENTS

This research was supported by the U.S. Department of Energy (DOE), Office of Biological and Environmental Research (BER), Subsurface Biogeochemical Research (SBR) Program through grant ER64172-1027487-001191 and the SBR Scientific Focus Area (SFA) at the Pacific Northwest National Laboratory (PNNL). Mössbauer spectroscopy measurements were performed at the William Wiley Environmental Molecular Sciences Laboratory (EMSL), a national scientific user facility sponsored by DOE-BER and located at PNNL, Richland, WA.

We thank J. Fredrickson (PNNL) for review of the manuscript.

REFERENCES

1. **Anderson CR, Pedersen K.** 2003. In situ growth of *Gallionella* biofilms and partitioning of lanthanides and actinides between biological material and ferric oxyhydroxides. Geobiology **1**:169–178.
2. **Bach W, Edwards KJ.** 2003. Iron and sulfide oxidation within the basaltic ocean crust: implication for chemolithoautotrophic microbial biomass production. Geochim. Cosmochim. Acta **67**:3871–3887.
3. **Bailey SW.** 1984. Crystal chemistry of the true micas. Rev. Mineral. Geochem. **13**:13–60.
4. **Banfield JF, Barker WW, Welch SA, Taunton A.** 1999. Biological impact on mineral dissolution: application of the lichen model to understanding mineral weathering in the rhizosphere. Proc. Natl. Acad. Sci. U. S. A. **96**:3404–3411.
5. **Berner EK, Berner RA.** 1996. Global environment: water, air, and geochemical cycles. Prentice Hall, Upper Saddle River, NJ.
6. **Bhatnagara A, Sillanpääb M.** 2011. A review of emerging adsorbents for nitrate removal from water. Chem. Eng. J. **168**:493–504.
7. **Blöthe M, Roden EE.** 2009. Composition and activity of an autotrophic Fe(II)-oxidizing, nitrate-reducing enrichment culture. Appl. Environ. Microbiol. **75**:6937–6940.
8. **Boyle JR, Voight GK, Sawhney BL.** 1967. Biotite flakes: alteration by chemical and biological treatment. Science **155**:193–195.
9. **Brantley SL.** 2010. Rock to regolith. Nat. Geosci. **3**:305–306.
10. **Buss HL, et al.** 2005. The coupling of biological iron cycling and mineral weathering during saprolite formation, Luquillo Mountains, Puerto Rico. Geobiology **3**:247–260.
11. **Chaudhuri SK, Lack JG, Coates JD.** 2001. Biogenic magnetite formation through anaerobic biooxidation of Fe(II). Appl. Environ. Microbiol. **67**: 2844–2848.
12. **Fitton JG, Gill RCO.** 1970. The oxidation of ferrous iron in rocks during mechanical grinding. Geochim. Cosmochim. Acta **34**:518–524.
13. **Graham RC, Rossi AM, Hubbert KR.** 2010. Rock to regolith conversion: producing hospitable substrates for terrestrial ecosystems. GSA Today **20**: 4–9.
14. **Hartshorne RS, et al.** 2009. Characterization of an electron conduit between bacteria and the extracellular environment. Proc. Natl. Acad. Sci. U. S. A. **106**:22169–22174.
15. **Hobbie JE, Daley RJ, Jasper S.** 1977. Use of Nuclepore filters for counting bacteria by fluorescence microscopy. Appl. Environ. Microbiol. **33**:1225–1228.
16. **Lovley DR, Goodwin S.** 1988. Hydrogen concentrations as an indicator of the predominant terminal electron accepting reactions in aquatic sediments. Geochim. Cosmochim. Acta **52**:2993–3003.
17. **Muehe EM, Gerhardt S, Schink B, Kappler A.** 2009. Ecophysiology and the energetic benefit of mixotrophic Fe(II) oxidation by various strains of nitrate-reducing bacteria. FEMS Microbiol. Ecol. **70**:335–343.
18. **Nesbitt HW, Young GM.** 1984. Prediction of some weathering trends of plutonic and volcanic rocks based on thermodynamic and kinetic considerations. Geochim. Cosmochim. Acta **48**:1523–1534.
19. **Neubauer SC, Emerson D, Megonigal JP.** 2002. Life at the energetic edge: kinetics of circumneutral iron oxidation by lithotrophic iron-oxidizing bacteria isolated from the wetland-plant rhizosphere. Appl. Environ. Microbiol. **68**:3988–3995.
20. **Pedersen K.** 1997. Microbial life in deep granitic rock. FEMS Microbiol. Rev. **20**:399–414.
21. **Rancourt DG, et al.** 1994. Determination of accurate [4]Fe^{3+}, [6]Fe^{3+}, and [6]Fe^{2+} site populations in synthetic annite by Mössbauer spectroscopy. Am. Mineral. **79**:51–62.
22. **Rancourt DG, Ping JY.** 1991. Voigt-based methods for arbitrary-shape static hyperfine parameter distributions in Mössbauer spectroscopy. Nuclear Instrum. Methods Phys. Res. B **58**:85–97.
23. **Sahl JW, et al.** 2008. Subsurface microbial diversity in deep-granitic-fracture water in Colorado. Appl. Environ. Microbiol. **74**:143–152.
24. **Schaefer MV, Gorski CA, Scherer MM.** 2011. Spectroscopic evidence for interfacial Fe(II)-Fe(III) electron transfer in a clay mineral. Environ. Sci. Technol. **45**:540–545.
25. **Schrenk MO, Huber JA, Edwards KJ.** 2010. Microbial provinces in the subseafloor. Annu. Rev. Mar. Sci. **2**:279–304.
26. **Scott AD, Amonette J.** 1988. Role of iron in mica weathering, p 537–623. *In* Stucki JW, Goodman BA, Schwertmann U (ed), Iron in soils and clay minerals. D. Reidel Publishing Company, Dordrecht, The Netherlands.
27. **Shelobolina ES, Gaw VanPraagh C, Lovley DR.** 2003. Use of ferric and ferrous iron containing minerals for respiration by *Desulfitobacterium frappieri*. Geomicrobiol. J. **20**:143–156.
28. **Sidborn M, Neretnieks I.** 2007. Long term redox evolution in granitic rocks: modelling the redox front propagation in the rock matrix. Appl. Geochem. **22**:2381–2396.
29. **Silverman MP.** 1979. Biological and organic chemical decomposition of silicates, p 445–465. *In* Trudinger PA, Swaine DJ (ed), Biogeochemical cycling of mineral-forming elements. Elsevier, Amsterdam, The Netherlands.
30. **Sobolev D, Roden EE.** 2004. Characterization of a neutrophilic, chemolithoautotrophic Fe(II)-oxidizing β-proteobacterium from freshwater wetland sediments. Geomicrobiol. J. **21**:1–10.
31. **Straub KL, Benz M, Schink B, Widdel F.** 1996. Anaerobic, nitrate-dependent microbial oxidation of ferrous iron. Appl. Environ. Microbiol. **62**:1458–1460.
32. **Stucki JW.** 1981. The quantitative assay of minerals for Fe^{2+} and Fe^{3+} using 1,10-phenanthroline. II. A photochemical method. Soil Sci. Soc. Am. J. **45**:638–641.
33. **Weber K, Picardal F, Roden E.** 2001. Microbially catalyzed nitrate-dependent oxidation of biogenic solid-phase Fe(II) compounds. Environ. Sci. Technol. **35**:1644–1650.
34. **Weed SB, Davey CB, Cook MG.** 1969. Weathering of mica by fungi. Soil Sci. Soc. Am. Proc. **33**:702–706.
35. **White AF, Yee A.** 1985. Aqueous oxidation-reduction kinetics associated with coupled electron cation transfer from iron-containing silicates at 25 degrees C. Geochim. Cosmochim. Acta **49**:1263–1275.
36. **Whitman WB, Coleman DC, Wiebe WJ.** 1998. Prokaryotes: the unseen majority. Proc. Natl. Acad. Sci. U. S. A. **95**:6578–6583.
37. **Wilson MJ.** 2004. Weathering of the primary rock-forming minerals: processes, products and rates. Clay Miner. **39**:233–266.